POLYMORPHIC PHASE BEHAVIOR OF PLATELET-ACTIVATING FACTOR

C. HUANG, J. T. MASON, F. A. STEPHENSON, AND I. W. LEVIN
Department of Biochemistry, University of Virginia School of Medicine, Charlottesville, Virginia; and the Laboratory of Chemical Physics, National Institute of Arthritis, Diabetes, and Digestive and Kidney Diseases, National Institutes of Health, Bethesda, Maryland

ABSTRACT Vibrational Raman and ^{31}P NMR spectroscopic experiments have been performed as a function of temperature on aqueous dispersions of 1-0-octadecyl-2-acetoyl-*sn*-glycero-3-phosphocholine, a chemically synthesized platelet-activating factor. In the temperature range of -7 to 30°C, the C(18)/PAF-H_2O system is shown, upon heating, to undergo two thermal phase transitions centered at 9.2° and 18.4°C. The low temperature transition, attributed to the interdigitated lamellar gel (II)→gel (I) phase transition, is characterized by the breakdown of large lamellar organizations into small, but aggregated, bilayer vesicles. The high-temperature transition corresponds to the interdigitated lamellar gel (I)→micellar transition. The molecular ordering and packing structure of C(18)/PAF in the two lamellar phases and phase transition regions are described. It appears that the interdigitated lamellar gel (I) phase is unique for C(18)/PAF dispersions when compared with the behavior of other chemically closely related phospholipids in excess water.

INTRODUCTION

Platelet-activating factor (PAF), a class of cell-derived autacoids, has been recognized recently to act as a potent mediator for acute allergic and inflammatory manifestations (Pinkard et al., 1982). Two chemically synthesized phospholipids, 1-0-hexadecyl-2-acetoyl-*sn*-glycero-3-phosphocholine [C(16)/PAF] and 1-0-octadecyl-2-acetoyl-*sn*-glycero-3-phosphocholine [C(18)/PAF], have been identified as constituting the natural PAF derived from rabbit basophils (McManus et al., 1983). These two biologically significant phospholipids are structurally highly asymmetrical. Moreover, they differ markedly from the common phosphoglycerides isolated from plasma membranes in that not only is the substituent at C-1 of the glycerol backbone a long saturated alkyl ether, which has either 16 or 18 carbon atoms, but also the acyl chain ester-linked at the *sn*-2 position is a short acetoyl chain that has only two carbon atoms.

Although extensive biological studies have been carried out to delineate the widely diverse pathophysiological activities provoked by PAF (Pinkard, 1983; Benveniste and Vargaftig, 1983), very little is known about the physical behavior of PAF in aqueous media. Recently, various lamellar and micellar phases and their associated thermal transitions have been observed for 1-stearoyllysophosphatidylcholine (C[18]/lysoPC) and 1-stearoyl-2-acetoyl-*sn*-glycero-3-phosphocholine (C[18]/C(2)PC) assemblies, in excess water (Wu et al., 1982; Huang et al., 1984). These phospholipids are chemically closely related to C(18)/PAF; however, they are incapable of eliciting symptoms of acute allergy and inflammation. Physical studies of C(18)/PAF dispersions as a function of temperature will provide useful information on the phase behavior of C(18)/PAF in excess water and will allow a comparison of fully hydrated PAF with other closely related phospholipids, such as C(18)/lysoPC and C(18)/C(2)PC. Such information may lead to a better understanding of the role of PAF in modulating potent allergic and inflammatory responses.

The aim of this work is to characterize the various phases and their associated thermal transitions for C(18)/PAF dispersions using both vibrational Raman and ^{31}P nuclear magnetic resonance spectroscopy as complementary physical techniques.

MATERIALS AND METHODS

Materials

Synthetic C(18)/PAF was purchased from Bachem, Inc., Torrance, CA. To remove possible trace amounts of fluorescent contaminants and other impurities in the commerical product, the synthetic phospholipid was further subjected to Folch's extraction (Folch et al., 1957). Briefly, the dry lipid sample was first allowed to dissolve completely in a 2:1 chloroform-methanol mixture. An aqueous buffer solution containing 5 mM EDTA and 10 mM Tris, pH 8.1, was added; after shaking the

[1] *Abbreviations used in this paper*: C(18)/PAF, 1-0-octadecyl-2-acetoyl-*sn*-glycero-3-phosphocholine; C(18)/C(2)PC, 1-stearoyl-2-acetoyl-*sn*-glycero-3-phosphocholine; C(18)/lysoPC, 1-stearoyl-*sn*-glycero-3-phosphocholine; diC(14)PC, L-α-dimyristoyl-*sn*-glycero-3-phosphocholine; diC(16)PC, L-α-dipalmitoyl-*sn*-glycero-3-phosphocholine; diC(18)PC, L-α-distearoyl-*sn*-glycero-3-phosphocholine; diC(22)PC, L-α-dibehenoyl-*sn*-glycero-3-phosphocholine; C(18)/C(14)PC, 1-stearoyl-2-myristoyl-*sn*-glycero-3-phosphocholine; $\Delta\sigma$, the chemical shift anisotropy.

mixture vigorously it was allowed to form a biphasic system. The lower lipid-containing phase was retained, and the chloroform-methanol solvent was removed by evaporation in a rotary evaporator. After drying, the C(18)/PAF was recrystallized twice from acetone-chloroform (95:5) at 20°C. The C(18)/PAF was then lyophilized from dry benzene followed by a second lyophilization from distilled, deionized water. The white C(18)/PAF powder was then stored at −20°C in a desiccator until used. All organic solvents were of spectroscopic grade, while the other chemicals used were of reagent grade.

Sample Preparation

For Raman measurements, 6–10 mg of lyophilized C(18)/PAF was dispersed in an appropriate volume of 75 mM NaCl-7.5 mM phosphate buffer solution, pH 7.0, to form a sample with a lipid concentration of 33.3% (wt/wt) in a final aqueous solution of 50 mM NaCl-5 mM phosphate buffer. The transparent lipid dispersion (10–15 μl) was micropipetted, at room temperature, into a Kimax glass capillary tube (1.25 mm i.d.) and then hermetically sealed. After the capillary was spun in a bench-top clinical centrifuge at room temperature, the sample was allowed to anneal at 0°C for a minimum of 1 mo before use. At 0°C, the lipid sample transforms from a clear solution into an opaque suspension.

For ^{31}P NMR measurements, an aqueous C(18)/PAF dispersion (125 mM) was prepared in 50 mM NaCl, 5 mM EDTA with 10 mM Tris buffer at pH 8.1. The sample, in a 10-mm NMR tube, was first warmed to 25°C to form a clear solution and then annealed at 0°C for 24 h to yield a white, opaque suspension. After the freeze-thaw cycle had been repeated three more times, the sample was stored at 0°C for 25 h before being incubated at −18°C for 72 h. It was then placed into the spectrometer's sample cavity, which had been thermally pre-equilibrated at 0°C. A thermal equilibration time of at least 1 h was allowed for the lipid sample before data acquisition. Succeeding experiments at ascending temperatures were performed by leaving the sample tube in the spectrometer for a minimum of 30 min equilibration at each temperature. In the 10 mm NMR tube a capillary tube (2 mm i.d.) containing $CDCl_3$ was used as an external field/frequency lock.

Raman Spectroscopy

Vibrational Raman spectra were obtained with a scanning Spex Ramalog 6 spectrometer equipped with holographic gratings and interfaced to a data acquisition system (model NIC-1180; Nicolet Computer Graphics, Martinez, CA), as previously described in detail (Huang et al., 1982). In general, Raman spectra were recorded at a scanning rate of 1 cm^{-1}/s with a laser excitation power, at 514.5 nM, of 200–220 mW at the sample. The lipid sample, which had been annealed at 0°C for more than a month, was incubated within the thermostatically controlled mount along the optical pathway for a minimum of 1 h at −10°C before Raman scans. Temperature profiles were then recorded in an ascending temperature mode; the sample was heated in 2°C increments with 12 min equilibration time at each temperature before recording the spectrum. With the scanning spectrometer, three to four signal averaged spectral scans in the vibrational C–H stretching region (2,800–3,100 cm^{-1}) were acquired at each temperature. The Raman spectral intensity ratios, I(2,932 cm^{-1})/I(2,882 cm^{-1}) and I(2,847 cm^{-1})/I(2,882 cm^{-1}), were used as indices for monitoring the order/disorder changes in the lipid assembly as a function of temperature.

^{31}P NMR Spectroscopy

All phosphorus NMR spectra of C(18)/PAF dispersions were obtained at 24.15 MHz using quadrature detection with a JEOL-FX60Q (Peabody, MA) Fourier-transform spectrometer operating under continuous broadband proton noise-decoupling at a power of 5 W, as described before (Huang et al., 1984). A 4,000-Hz sweep width was used, and 4,000 data points were collected with 400–10,000 scans accumulated per spectrum at a delay of 1 s between pulses. A line broadening of either 10 or 5 Hz was introduced during signal enhancement for the broad asymmetrical lineshapes and the narrow isotropic signals, respectively.

RESULTS

Thermal Phase Transitions of C(18)/PAF as Detected by Raman Spectroscopy in the 2,800–3,100 cm^{-1} Stretching Mode Region

Representative Raman spectra of C(18)/PAF dispersions in the 2,800–3,100 cm^{-1} C–H stretching mode region recorded at −6°, 12.9°, and 24.7°C are shown in Fig. 1. The vibrationally congested 2,800–3,100 cm^{-1} spectral region consists of a number of vibrational transitions whose assignments have been discussed in detail elsewhere (Huang et al., 1982; Levin, 1984). It is worth mentioning that the two dominant features at ~2,848 and 2,882 cm^{-1} correspond mainly to the symmetric and the asymmetric C–H stretching modes, respectively, for the coupled methylene moieties of the hydrocarbon chains in the bilayer

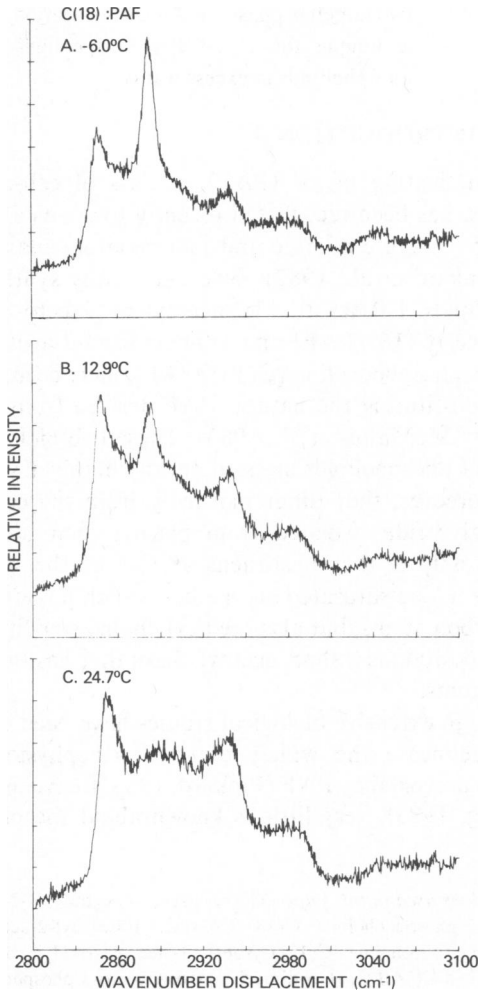

FIGURE 1 Raman spectra of C(18)/PAF dispersions in the 2,800–3,100 cm^{-1} C–H stretching mode region recorded at (*A*) −6°C, (*B*) 12.9°C, and (*C*) 24.7°C.

interior; smaller relative peak-height intensity ratios, I(2,848 cm^{-1})/I(2,882 cm^{-1}), reflect stronger lateral chain-chain interactions in the bilayer. The broad feature centered at ~2,935 cm^{-1} originates, in part, from a Fermi resonance component of the symmetric C–H stretching modes of the hydrocarbon chain terminal methyl groups; the peak-height intensity at 2,935 cm^{-1} is more prominent when the intrachain conformation disorder and the lattice packing disorder are increased in the hydrocarbon region of the lipid assembly. In general, higher I(2,935 cm^{-1})/I(2,882 cm^{-1}) intensity ratios can be attributed to a greater lattice and conformational disorder present in the hydrocarbon region of the lipid assembly. Consequently, the relative peak-height intensity ratios, (I[2,935 cm^{-1}]/I[2,882 cm^{-1}]) and (I[2,848 cm^{-1}]/I[2,882 cm^{-1}]), are widely used as Raman spectral indices to monitor the hydrocarbon chain order/disorder changes exhibited by lipid assemblies undergoing multiple thermal phase transitions (Huang et al., 1984; Huang et al., 1982).

Fig. 2 *A* displays the temperature profile derived from the I(2,935 cm^{-1})/I(2,882 cm^{-1}) peak-height intensity ratio for C(18)/PAF dispersions. Upon raising the sample temperature from −7° to 30.5°C, our data clearly reveal two sharp discontinuities centered at 9.2° and 18.4°C, respectively. These two discontinuities in the Raman spectral index reflect two abrupt increases both in the chain and lattice disorder of the C(18)/PAF assembly. We interpret the discontinuities observed in Fig. 2 *A* to be due to the thermotropic phase transitions occurring in the aqueous dispersion of C(18)/PAF.

The lower temperature transition detected in Fig. 2 *A* is assigned to a solid-solid or gel (II)–gel (I) phase transition on the basis of the magnitude of Raman peak-height intensity ratios, I(2,935 cm^{-1})/I(2,882 cm^{-1}), in the temperature interval of −7 to 16°C. Below T_m, the lower phase transition temperature (9.2°C), the value of the Raman spectral index, I(2,935 cm^{-1})/I(2,882 cm^{-1}), for C(18)/PAF dispersions increases only slightly with increasing temperatures. At 10°C below T_m, the value of I(2,935 cm^{-1})/I(2,882 cm^{-1}) is 0.33, a value that has also been observed for lamellar dibehenoylphosphatidylcholine ((diC[22]PC)) in the gel state at the same reduced temperature (Huang et al., 1982). It is pertinent to mention that this value of 0.33 is smaller than the value of 0.39 obtained for distearoylphosphatidylcholine multibilayers in the gel state at the corresponding reduced temperature (Huang et al., 1982). Since the spectral index of I(2,935 cm^{-1})/I(2,882 cm^{-1}) is indicative of both the intrachain conformational disorder and lattice packing disorder (Levin, 1984), our results imply that the hydrocarbon chains of C(18)/PAF in the lipid assembly at temperatures below T_m are packed more or less identically with those of diC(22)PC in the gel state; however, they are more ordered than the acyl chains of the gel-state bilayer characteristic of distearoylphosphatidylcholine molecules. Over a very narrow temperature region across T_m, the Raman spectral index of I(2,935 cm^{-1})/I(2,882 cm^{-1}) increases abruptly from 0.36 at 9.1°C to an average value of 0.55 at 9.6°C, demonstrating that the hydrocarbon chains of C(18)/PAF undergo a cooperative order/disorder phase transition

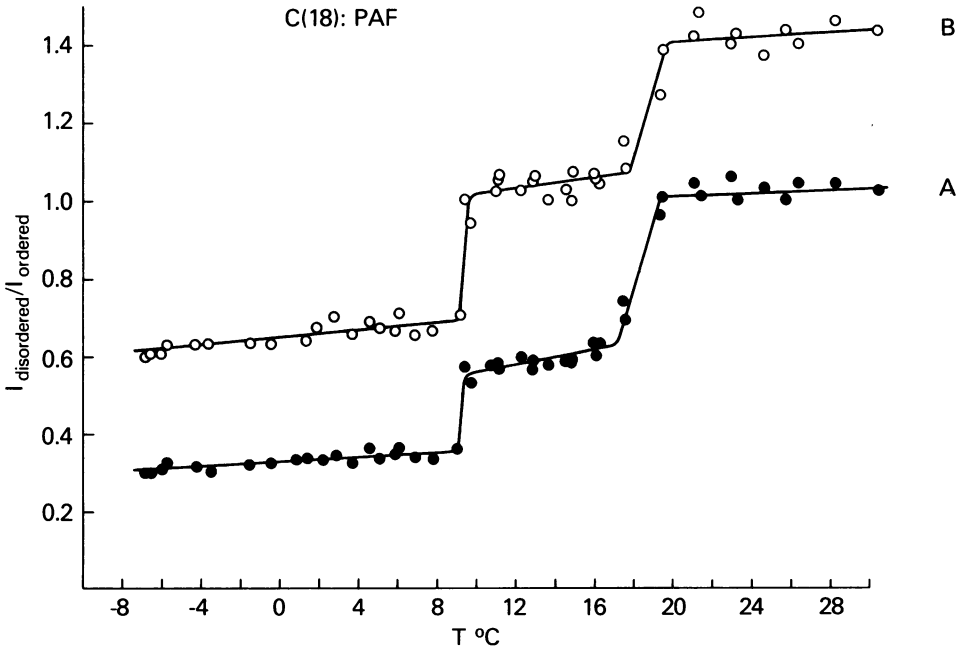

FIGURE 2 Temperature profiles for C(18)/PAF dispersions using (*A*) the Raman spectral I(2,935 cm^{-1})/I(2,882 cm^{-1}) peak-height intensity ratio (•) and (*B*) the I(2,848 cm^{-1})/I(2,882 cm^{-1}) peak-height intensity ratio (o) as Raman order/disorder indices reflecting the structures and the thermal phase transitions of the phospholipid assembly in excess water.

across a narrow 0.5°C temperature range. The abrupt rise in I(2,935 cm^{-1})/I(2,882 cm^{-1}) on heating the lipid sample is attributed to a simultaneous increase in the number of *gauche* conformers in the lipid chains and decrease in lateral chain-chain interactions. It is interesting to note that the I(2,935 cm^{-1})/I(2,882 cm^{-1}) intensity ratio of 0.55 for C(18)/PAF dispersions at the completion temperature of the lower temperature phase transition may be contrasted with a much larger, characteristic value of 0.81 observed for saturated symmetric phospholipids, such as diC(16)PC, in the highly disordered liquid-crystalline state (Huang et al., 1982). This value of 0.55, however, is extremely close to the value of 0.56 for the I(2,935 cm^{-1})/I(2,882 cm^{-1}) ratio observed for C(18)/C(14)PC dispersions at the onset temperature of the gel to liquid-crystalline phase transition (Huang et al., 1983). From these Raman data we conclude that the lower temperature phase transition depicted in Fig. 2 *A* represents a solid-solid or gel (II)–gel (I) phase transition.

As the temperature is raised above the low-temperature C(18)/PAF gel (II)–gel (I) phase transition, the Raman spectral ratio of I(2,935 cm^{-1})/I(2,882 cm^{-1}) increases gradually and linearly with increasing temperature to at least 16°C. As the lipid sample is heated further above 17°C, a second abrupt increase in the I(2,935 cm^{-1})/I(2,882 cm^{-1}) Raman spectral index is observed to take place within 2°–2.5°C (Fig. 2 *A*). The magnitudes of I(2,935 cm^{-1})/I(2,882 cm^{-1}) for C(18)/PAF at temperatures above the completion temperature of the high-temperature phase transition (19.4°C) are relatively constant, with an average value slightly greater than unity; they are very similar to the observed values for C(18)/lysoPC in the micellar state (Wu et al., 1982). Consequently, we interpret the high-temperature phase transition detected in Fig. 2 *A* as the gel (I) to micellar transition for C(18)/PAF dispersions.

The temperature profile constructed from an alternate peak-height intensity ratio, I(2,848 cm^{-1})/I(2,882 cm^{-1}), is shown in Fig. 2 *B* for C(18)/PAF dispersions. This ratio, or spectral index, reflects the lateral chain-chain interactions in a lipid assembly that are perhaps less perturbed by intrachain conformational changes (Levin, 1984; Huang et al., 1983; Snyder et al., 1978). The temperature profile shows clearly two discontinuities; moreover, it runs virtually parallel to the curve reflecting the temperature dependence of the I(2,935 cm^{-1})/I(2,882 cm^{-1}) spectral ratios.

Carbonyl Stretching Region (1,650–1,750 cm^{-1}) and CH_2 Deformation Region (1,350–1,550 cm^{-1})

Fig. 3 shows the Raman carbonyl stretching region for C(18)/PAF dispersions. The temperature of the phospholipid sample is −4.7°C, which is far below the low-temperature phase transition temperature. The spectrum

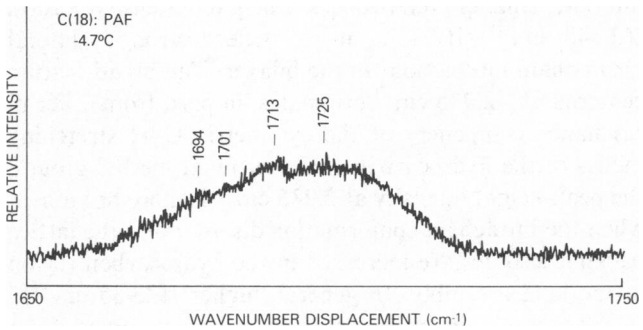

FIGURE 3 Raman spectra of C(18)/PAF dispersions at −4.7°C in the carbonyl stretching mode region (1,650–1,750 cm^{-1}).

of this weak feature represents an accumulation of 399 scans recorded at 1 cm^{-1} s^{-1}. A single broad Raman C═O stretch band centered at ~1,720 cm^{-1} is observed with a suggestion of superimposed weak vibrational transitions appearing toward low frequencies. The bandwidth at half peak-height of the broad C═O related band is 39 cm^{-1}.

The Raman spectrum of C(18)/PAF dispersions at −6.5°C in the methylene deformation region (1,350–1,550 cm^{-1}) is depicted in Fig. 4. The methylene deformation modes are clearly observed at 1,438 and 1,457 cm^{-1}. Raman spectra of similar lineshape have been observed for diC(14)PC and diC(16)PC in aqueous dispersions in the gel state (Levin, 1984; Bush et al., 1980). Absence of a Raman characteristic feature ~1,420 cm^{-1}, at −6.5°C, in the methylene deformation region indicates that the hydrocarbon chains of C(18)/PAF at such a low temperature are not packed in either an orthohombic or monoclinic subcell (Boerio and Koenig, 1970).

Polymorphic Structure of C(18)/PAF as Detected by ^{31}P NMR

The 24.15 MHz proton-decoupled ^{31}P NMR spectra of C(18)/PAF dispersions, recorded at various temperatures, are presented in Fig. 5. The low-temperature spectra (0°–8°C) exhibit a broad powder-type pattern with a

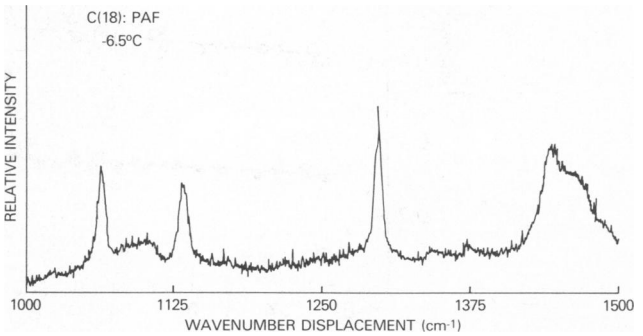

FIGURE 4 Raman spectrum of C(18)/PAF dispersions at −6.5°C in the 1,000–1,500 cm^{-1} region. The broad band with a high-field shoulder in the 1,400–1,500 cm^{-1} region is attributable to the chain methylene deformation modes.

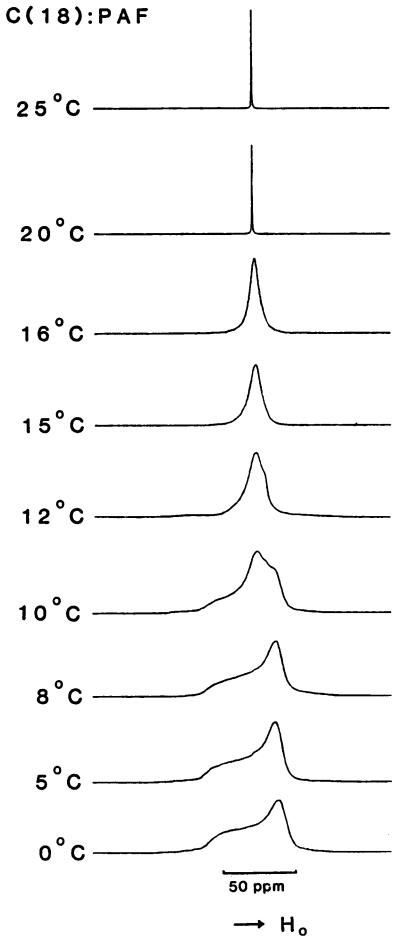

FIGURE 5 Proton noise-decoupled 24.15 MHz ^{31}P NMR spectra of aqueous dispersions of C(18)/PAF. The spectra were taken from the same sample (125 mM) and recorded in an ascending temperature mode; temperatures are indicated adjacent to respective spectra.

pronounced axially symmetric lineshape, known as the "bilayer" lineshape, which is characterized by a high-field peak with a broad low-field shoulder (Cullis and DeKruijff, 1978; Seelig, 1978). The chemical shift anisotropy, determined from the separation between the points of maximum slope in the low-field shoulder and the high-field peak, decreases slowly from 69 ppm at 0°C to 66 ppm at 5°C, and then to 62 ppm at 8°C. An axially symmetric spectrum with $\Delta\sigma = 69$ ppm has been observed for dipalmitoylphosphatidylcholine molecules in the gel-state bilayer at −10°C (Herzfeld et al., 1978). This limiting value of the chemical shift anisotropy can be explained quantitatively by a model for phospholipid dynamics that assumes essentially rapid (on the ^{31}P timescale) rotation of the phospholipid as a whole around the bilayer normal (Herzfeld et al., 1978; Smith and Ekiel, 1984). Such broad powder-type spectra observed at low temperatures are indicative of C(18)/PAF molecules packed in a bilayer organization; moreover, the value of $\Delta\sigma$ reflects that C(18)/PAF undergoes fast axial rotator motion around the normal to the lipid bilayer.

In the 10° and 12°C spectra of Fig. 5, the ^{31}P NMR lineshape of the prominent broad powder-type pattern is distorted near the central portion of the feature by an emerging narrower resonance. Moreover, the intensity of the central narrower resonance grows steadily with increasing temperature at the expense of the broad powder-type pattern. Above 12°C, the broad powder-type pattern collapses completely to a single, nearly symmetric peak with the value of the effective residual chemical shift anisotropy for the collapsed resonance estimated to be ~26 ppm. This presumably reflects the fact that in the narrow temperature interval of 10–12°C, C(18)/PAF molecules are in the thermotropic phase transition region where two different lipid organizations coexist, resulting in a superposition of two spectral lineshapes. This behavior of C(18)/PAF appears to be in good agreement with our Raman data presented in Fig. 2, except that the transition temperature based on the ^{31}P results is slightly higher.

At 15° and 16°C, C(18)/PAF dispersions exhibit a single nearly symmetric and narrower ^{31}P spectrum. The observed narrower lineshape ($\Delta\sigma \simeq 26$ ppm) reflects a larger angular amplitude of the axial rotation of the phosphate moiety of the lipid headgroup in the phospholipid assembly. This has been interpreted as being caused primarily by the additional motional averaging of the lipid headgroup as a result of rapid lateral diffusion of phospholipid molecules in the intermediate size range (400–1,500 Å in radius) of bilayer vesicles (Burnell et al., 1980). The change in ^{31}P NMR spectral pattern from a powder-type to a nearly symmetric type, shown in Fig. 5, indicates that the lower temperature phase transition detected in C(18)/PAF dispersions is coupled with the breakdown of the phospholipid organization from large lamellar structures to smaller intermediate-size vesicles.

At 20° and 25°C, the ^{31}P NMR spectra of C(18)/PAF dispersions are an isotropic line of 2-ppm width, indicative of C(18)/PAF in a state allowing complete motional averaging of the phosphorus chemical-shift tensor components. Although phospholipids in small vesicles, micelles, rhombic, and cubic phases are known to undergo isotropic motion ($\tau_c < 10^{-4}$) giving rise to sharp symmetric ^{31}P NMR signals (Cullis and DeKruijff, 1979), we conclude that C(18)/PAF molecules are organized in micelles at temperatures above the high temperature phase transition based on the Raman I(2,935 cm^{-1})/I(2,882 cm^{-1}) spectral index. The sharp, symmetric ^{31}P NMR line can, therefore, be attributed to the rapid Brownian tumbling or rotational motion of C(18)/PAF micelles in the aqueous medium and to the rapid diffusion of C(18)/PAF molecules in a highly fluctuating, disordered micellar state.

DISCUSSION

The combined vibrational Raman and ^{31}P NMR spectroscopic studies on aqueous dispersions of C(18)/PAF, a biologically significant phospholipid, demonstrate that the

phospholipid assembly, upon heating, undergoes two discernible phase transitions in the temperature range of −7 to 30°C. The thermal behavior of the lamellar phases and the phase transitions of C(18)/PAF are discussed below in terms of the assemblies' hydrocarbon chain packing characteristics and lipid motional behavior.

Gel (II) Phase or Fully Interdigitated Gel (II) Phase

At 10°C below the low-temperature phase transition temperature, the Raman spectral ratio, I(2,935 cm^{-1})/I(2,882 cm^{-1}), for C(18)/PAF dispersions is 0.33 (Fig. 2 *A*), which is the same as that for gel-state lamellar diC(22)PC obtained at a common reduced temperature (Huang et al., 1982). This value, however, is significantly less than the corresponding value of 0.39 obtained for gel-state lamellar diC(18)PC recorded at 10°C below its T_m (Huang et al., 1982). In the gel-state bilayer, diC(22)PC is expected to have a smaller value of the Raman spectral ratio, I(2,935 cm^{-1})/I(2,882 cm^{-1}), than that of diC(18)PC at the same reduced temperature. This smaller ratio, reflecting greater lateral chain-chain interactions and less intrachain conformational disorder, can be attributed, in part, to increased van der Waals interactions arising from the additional methylene moieties and to the relatively smaller perturbation of the molecular packing of the diC(22)PC acyl chains by the chain terminal methyl groups (Huang and Levin, 1983). This chain perturbation in bilayers has been quantitatively analyzed previously by a perturbation parameter, *P*, which is inversely related to the acyl chain length for saturated symmetric phospholipids (Mason and Huang, 1981).

Nearly identical agreement between the I(2,935 cm^{-1})/I(2,882 cm^{-1}) Raman spectral ratios obtained for C(18)/PAF dispersions in the gel (II) state and diC(22)PC dispersions in the gel state indicates that these two entirely different phospholipid species are very similarly packed. They both have strong lateral chain-chain interactions and a high degree of intrachain conformational order in their respective gel-state lamellae. The most likely packing arrangement that allows C(18)/PAF to be packed as orderly as diC(22)PC in the gel-state bilayer is one in which the highly asymmetric phospholipid molecules form an interdigitated bilayer. This model corresponds closely to the molecular packing arrangement suggested for C(18)/C(2)PC in the interdigitated gel phase (Huang et al., 1984). In the interdigitated gel-state bilayer, the short acetoyl chain linked to the C-2 atom of the phospholipid glycerol moiety runs parallel to the bilayer surface, while the long C(18)-hydrocarbon chain lies perpendicular to the bilayer surface and completely spans the entire hydrocarbon width of the bilayer (Huang et al., 1984).

An indication of the chain orientation and motion of the short *sn*-2 acetoyl chain is provided by the carbonyl stretching region of C(18)/PAF dispersions shown in Fig. 3. The Raman C═O stretch band at −4.7°C has one broad, asymmetric feature centered at ~1,720 cm^{-1} with a 39 cm^{-1} bandwidth at half peak-height. The Raman spectrum of fully hydrated C(18)/C(2)PC dispersions in the highly ordered crystalline phase was observed recently to display two clearly separable C═O stretching mode bands with nearly equal intensities and half-bandwidths (10.5 cm^{-1}) at 1,720 and 1,748 cm^{-1} (Huang et al., 1984.) The low- and high-frequency carbonyl stretching modes were assigned to the two phospholipid C═O bonds in the *sn*-2 and *sn*-1 acyl chain, respectively. The C(18)/PAF molecule, however, has only one carbonyl moiety at the ester linkage of the *sn*-2 acetoyl chain. The C═O stretching frequency of C(18)/PAF dispersions in the gel (II) state corresponds unequivocally to the *sn*-2 C═O stretching band in the crystalline C(18)/C(2)PC. This result is taken as strong evidence for the similarity of the average overall conformation and orientation of the short acetoyl chain in the gel (II)-state of C(18)/PAF to that of the *sn*-2 acetoyl chain in crystalline C(18)/C(2)PC. Since the *sn*-2 acetoyl chain of C(18)/C(2)PC in the highly ordered crystalline-state lamellae appears to lie parallel to the bilayer surface (Huang et al., 1984), we conclude that the acetoyl chains in the gel (II)-state of C(18)/PAF lamellae have an average overall orientation that is parallel to the bilayer surface, thus exposing the carbonyl group to the aqueous phase. The weak vibrational transitions observed at 1,694, 1,701, and 1,713 cm^{-1} are believed to represent small populations of carbonyl groups that are hydrogen bonded to water (Bush et al., 1980).

Although the C═O stretching frequency observed for C(18)/PAF dispersions in the gel (II)-state is virtually identical to that of the lower frequency C═O band of the two C═O stretches observed for C(18)/C(2)PC dispersions in the highly ordered crystalline state, the C(18)/PAF C═O band is considerably broader than the low-frequency C═O in the C(18)/C(2)PC spectrum. This band broadening can be attributed, in addition to hydrogen-bonded species, to a greater motional disorder of the acetoyl chain in the fully hydrated gel (II)-state C(18)/PAF bilayer, resulting in a greater distribution of chain rotational isomers about the average chain conformation.

The long C(18)-hydrocarbon chains of C(18)/PAF lamellae, in the gel (II)-state, most likely adopt a hexagonal lateral packing of the chain axes on the basis of the Raman spectral features observed in the methylene deformation region (1,400–1,500 cm^{-1}). As shown in Fig. 4, the methylene deformation region displays an overlapped feature with a sharp band at 1,438 cm^{-1} and a weak broad shoulder on the high frequency side. This Raman spectral pattern shown is closely similar to that exhibited by fully hydrated diC(14)PC or diC(16)PC in the gel-state bilayer (Bush et al., 1980). The zig-zag planes of the nearly all-*trans*, long acyl chains of these saturated symmetric phospholipids are known, in the gel bilayer state, to adopt a two-dimensional hexagonal packing with axial rotational disorder (Ruocco and Shipley, 1982).

The ^{31}P NMR spectra of C(18)/PAF dispersions in the low-temperature region (Fig. 5) display the standard axially symmetric feature, 62–69 ppm wide, characteristic of diC(16)PCs in the gel state (Herzfeld et al., 1978). This observation is consistent with the Raman result obtained in the deformation region just discussed above, indicating that the long C(18)-hydrocarbon chains in the interdigitated gel (II)-state of the C(18)/PAF bilayer undergo random rotational motions about the chain axes.

Lower Temperature Transition or Gel (II)-Gel (I) Transition

From the magnitude of the Raman spectral ratio, I(2,935 cm^{-1})/I(2,882 cm^{-1}), for C(18)/PAF dispersions in the temperature interval of $-7°$ to 16°C, we associate the 9.2°C low-temperature transition of Fig. 2 with a solid-solid or gel (II)-gel (I) phase transition. On passing through the low temperature transition, ^{31}P NMR spectra of C(18)/PAF dispersions at 10° and 12°C clearly show the transformation of a predominant, broad, powder-type feature with a large negative chemical shift anisotropy ($\Delta\sigma$ = 62 ppm) to a broadened feature coexisting with one of narrower spectral width ($\Delta\sigma$ = 38 ppm) over a very brief temperature interval (Fig. 5). The composite ^{31}P spectrum indicates the coexistence of the two different lipid organizations in the gel (I) and (II) phases during the low-temperature phase transition. The asymmetrically broadened powder-type pattern with $\Delta\sigma \cong 62$ ppm can be attributed to a rotator motion of the whole C(18)/PAF molecule around its long axis in the bilayer. This rotational averaging results in the projection of the anisotropic shielding along the rotation axis, which, in turn, leads to a ^{31}P NMR lineshape characteristic of gel-state diacyl phospholipids packed in a large (radius $\geq$ 2,500 Å) bilayer structure (Herzfeld et al., 1978; Burnell et al., 1980; Smith and Ekiel, 1984). The superimposed narrower peak ($\Delta\sigma$ = 26 ppm) can be explained by either a change in phosphocholine headgroup conformation (Thayer and Kohler, 1981) or by the breakdown of large lamellar structures into medium-sized vesicles (Burnell et al., 1980). It has been shown that a rotation of the phosphocholine headgroup in a bilayer away from a parallel orientation to a more perpendicular configuration will result in a narrowing of the symmetric ^{31}P NMR bilayer spectrum (Thayer and Kohler, 1981). However, due to intermolecular interactions the phosphocholine P–N dipole appears to be oriented parallel to the bilayer surface, in the absence of polyvalent ions, in virtually all systems investigated to date irrespective of the degree of hydration (Hauser et al., 1981), the configurational state of the acyl chains (Büldt et al., 1979) or the morphology of the phospholipid assemblies (Yeagle et al., 1975; Seelig and Seelig, 1980). Thus, there is currently no evidence for the existence of phospholipid headgroup conformational changes. Hence, we believe that the superimposed narrower peak appears to arise principally from phospholipids packed in medium-sized (400–1,500 Å in radius) vesicles (Burnell et al., 1980). In these vesicles additional rapid lateral diffusions of the lipid molecules are coupled with the axially symmetric motion in the medium-size vesicles, leading to the reduction in the chemical shift anisotropy (Burnell et al., 1980). These results suggest that the abrupt increase in both the interchain and the intrachain disorder in C(18)/PAF lamellae which occurs on heating the lipid assembly through the low-temperature transition may be responsible for inducing the breakdown of large C(18)/PAF lamellar structures into medium-size vesicles.

Similar breakdowns of large multilamellar liposomes into smaller vesicular structures during the gel (II)→gel (I) phase transition were observed with other asymmetric phospholipids, such as sphingomyelins and C(18)/C(14)PC by ^{31}P NMR and freeze-fracture electron microscopy (Hui et al., 1980; Hui et al., 1984). The size alteration of the liposomes at the gel (II)→gel (I) phase transition probably arises as a result of the special geometry or shape of the asymmetric phospholipid molecules that favor, in the gel (I) state, a self-assembly into structures of relatively higher surface curvature, such as medium-size vesicles. Results from dynamic light scattering (Mason and Huang, unpublished experiments) indicate that the effective size of the C(18)/PAF assemblies remains large, in the range of 10^4 Å, in the gel (I) phase. In addition, solutions of the C(18)/PAF assemblies are translucent and highly viscous with a gelatin-like consistency. To reconcile these observations with the results from ^{31}P NMR, we propose that the C(18)/PAF medium-sized bilayer vesicles are highly aggregated in an extensive three dimensional matrix in aqueous solution within the gel (I) phase. The morphology of this phase is currently under investigation.

Gel (I) Phase

Between the two phase transition temperatures, C(18)/PAF molecules are packed in medium-size, albeit aggregated, bilayer vesicles. The range of vesicle sizes needs to be determined by other physical techniques. Nevertheless, based on Raman data from Fig. 2, C(18)/PAF molecules are considered to be packed in a gel state that is considerably more ordered than the liquid-crystalline state observed for symmetric diacyl phospholipids in noninterdigitated bilayers at temperatures above T_m. It is likely that asymmetric C(18)/PAF molecules are packed in an interdigitated gel-state bilayer. This interdigitated gel state, which we call the gel (I) phase, is significantly more disordered than the interdigitated gel (II) state discussed earlier.

In general, at various temperatures the acyl chains of phospholipids exhibit an order parameter "plateau" followed by a decrease near the chain methyl terminus in the bilayer center (Brown et al., 1979). It is thus reasonable to postulate the major difference between the interdigitated

C(18)/PAF gel (I) and gel (II) states lies in the degree of ordering of lipid chains in the hydrocarbon region of the bilayer. In the gel (I) state, more *gauche* conformers can be assumed to be present in the C(18)-hydrocarbon chain, leading to a weaker chain-chain interaction in the lipid assembly. Heating causes the introduction of *gauche* conformers, which affect the overall shape or geometry of the lipid molecules and result in the breakdown of large lamellar structures into smaller vesicles. The weaker chain-chain interaction and the smaller size of the vesicle result in an increased lateral diffusion of each C(18)/PAF molecule in the lipid vesicle. This diffusion is superimposed on the rotational motion of the entire lipid molecule about its long molecular axis; consequently, a narrower ^{31}P NMR signal for C(18)/PAF dispersions at temperatures between the two phase transitions is observed.

Higher Temperature Transition or Gel (I) — Micellar Transition

The number of *gauche* bonds introduced into the C(18)-hydrocarbon chain of C(18)/PAF in the gel (I) state can be considered to increase progressively with increasing temperature. At the critical temperature corresponding to the high-temperature phase transition temperature, the increased intrachain disordering caused by the presence of a relatively large number of *gauche* bonds becomes large enough to allow C(18)/PAF dispersions to transform from the gel (I) state to the highly disordered micellar state.

A sharp cooperative lamellar-micellar transition centered at 26.2°C was demonstrated for C(18)-lysophosphatidylcholine assemblies, in excess water, by quasi-elastic light scattering, Raman spectroscopy, electron microscopy, and high-sensitivity differential scanning calorimetry (Wu et al., 1982). More recently, a similar transition for aqueous C(18)/C(2)PC dispersions with a transition temperature of 18.5°C was observed by Raman and ^{31}P NMR techniques (Huang et al., 1984). The present work shows that the gel (I) micellar transition takes place at 18.4°C for C(18)/PAF dispersions. The nearly identical transition temperatures (T_m) for C(18)/C(2)PC and C(18)/PAF dispersions may be fortuitous. Nevertheless, it is possible that although the average molecular packing of C(18)/PAF in medium-size vesicles is apparently different from that of C(18)/C(2)PC in multilamellar bilayers, the packing difference is compensated energetically by changes in phospholipid subclasses when the C-1 ether bond in PAF is replaced by an ester linkage in C(18)/C(2)PC, leading to the similarities in the observed T_ms.

A comparison of the results obtained for C(18)/PAF dispersions and those observed for highly asymmetric C(18)/lysoPC and C(18)/C(2)PC dispersions (Wu et al., 1982; Huang et al., 1984) is worth further consideration. C(18)/lysoPC molecules form extended interdigitated multilamellar structures in excess water at 0°C. The lamellar structure of C(18)/lysoPC is highly ordered, similar to the highly ordered gel (II) state observed for C(18)/PAF. The highly ordered C(18)/lysoPC lamellae, however, undergo a single phase transition from the lamellar to micellar form when heated above a temperature of 26°C. At 0°C, C(18)/C(2)PC molecules also form interdigitated lamellae, in excess of water. Unlike C(18)/lysoPC, C(18)/C(2)PC lamellae undergo two phase transitions at 6.2° and 18.5°C, which can be described by the following scheme: interdigitated crystalline phase⟶interdigitated gel phase⟶micellar phase (Huang et al., 1984). The present study also shows two phase transitions for C(18)/PAF dispersions. There are, however, some quantitative differences. The crystalline phase is not observed for C(18)/PAF in the temperature interval between 0°C and the first phase transition temperature. We cannot rule out the possibility that C(18)/PAF molecules may pack into the interdigitated crystalline phase at temperatures below −18°C. We do know, however, that C(18)/PAF moelcules can form gel (I) and gel (II) phases. A potentially significant finding is that the characteristic organization of the gel (I) phase for C(18)/PAF is not observed in either C(18)/lysoPC or C(18)/C(2)PC assemblies. In this phase, C(18)/PAF molecules are packed in a lamellar structure with a relatively small radius of curvature. Furthermore, the lateral chain-chain interactions for C(18)/PAF molecules in the gel (I) phase are far weaker than those observed for C(18)/lysoPC and C(18)/C(2)PC in the gel state.

At this juncture it would appear that PAF elicits its pathophysiological responses by interaction with specific cell surface receptors (Hwang et al., 1983). However, the physical properties of PAF are still of considerable importance and may dictate the behavior of PAF in membranes as well as the interaction between PAF and its membrane receptor. We have presented evidence here that C(18)/PAF molecules are packed in lamellar structures with a relatively small radius of curvature in the gel (I) phase. This might indicate that PAF is capable of destabilizing the normal extended lamellar packing within its immediate microenvironment in biological membranes or that PAF may preferentially partition into regions of high surface curvature within membranes. Whether these properties of PAF are related to its biological activity will obviously require further investigation.

This work was supported, in part, by National Institutes of Health grant GM-17452.

Received for publication 3 June 1985 and in final form 19 September 1985.

REFERENCES

Benveniste, J., and B. B. Vargaftig. 1983. Platelet-activating factor: an ether lipid with biological activity. *In* Ether Lipids: Biochemical and Biomedical Aspects. H. K. Mangold and F. Paltauf, editors. Academic Press, Inc., New York.

Boerio, F. S., and J. L. Koenig. 1970. Raman scattering in crystalline polyethylene. *J. Chem. Phys.* 52:3425–3431.

Brown, M. F., J. Seelig, and U. Haeberlen. 1979. Structural dynamics in

phospholipid bilayers from deuterium spin-lattice relaxation time measurements. *J. Chem. Phys.* 70:5045–5053.

Büldt, G., H. U. Gally, J. Seelig, and G. Zaccai. 1979. Neutron diffraction studies on phosphatidylcholine model membranes. I. Head group conformation. *J. Mol. Biol.* 134:673–691.

Burnell, E. E., P. R. Cullis, and B. DeKruijff. 1980. Effects of tumbling and lateral diffusion on phosphatidylcholine model membrane ^{31}P-NMR lineshapes. *Biochim. Biophys. Acta.* 603:63–69.

Bush, S. F., R. G. Adams, and I. W. Levin. 1980. Structural reorganizations in lipid bilayer systems: effect of hydration and sterol addition on Raman spectra of dipalmitoylphosphatidylcholine multilayers. *Biochemistry.* 19:4429–4436.

Cullis, P. R., and B. DeKruijff. 1978. The polymorphic phase behavior of phosphatidylethanolamines of natural and synthetic origin. *Biochim. Biophys. Acta.* 513:31–42.

Cullis, P. R., and B. DeKruijff. 1979. Lipid polymorphism and the functional roles of lipids in biological membranes. *Biochim. Biophys. Acta.* 559:399–420.

Folch, J., M. Lees, and C. H. Sloane-Stanley. 1957. A simple method for the isolation and purification of total lipids from animal tissue. *J. Biol. Chem.* 226:497–509.

Hauser, H., I. Pascher, R. H. Pearson, and S. Sundell. 1981. Preferred conformation and molecular packing of phosphatidylethanolamine and phosphatidylcholine. *Biochim. Biophys. Acta.* 650:21–51.

Herzfeld, J., R. G. Griffin, and R. H. Haberkorn. 1978. Phosphorous-31 chemical shift tensors in barium diethyl phosphate and urea-phosphoric acid: model compounds for phospholipid headgroups. *Biochemistry.* 17:2711–2722.

Huang, C., J. R. Lapides, and I. W. Levin. 1982. Phase transition behavior of saturated, symmetric chain phospholipid bilayer dispersions determined by Raman spectroscopy: correlation between spectral and thermodynamic parameters. *J. Am. Chem. Soc.* 104:5926–5930.

Huang, C., and I. W. Levin. 1983. Effect of lipid chain length inequivalence on the packing characteristics of bilayer assemblies. Raman spectroscopic study of phospholipid dispersions in the gel state. *J. Phys. Chem.* 87:1509–1513.

Huang, C., J. T. Mason, and I. W. Levin. 1983. Raman spectroscopic study of saturated mixed chain phosphatidylcholine multilamellar dispersions. *Biochemistry.* 22:2775–2780.

Huang, C., J. T. Mason, F. A. Stephenson, and I. W. Levin. 1984. Raman and ^{31}P NMR spectroscopic identification of a highly ordered lamellar phase in aqueous dispersions of 1-stearoyl-2-acetyl-*sn*-glycero-3-phosphorylcholine. *J. Phys. Chem.* 88:6454–6458.

Hui, S. W., J. T. Mason, and C. Huang. 1984. Acyl chain interdigitation in saturated mixed chain phosphatidylcholine bilayer dispersions. *Biochemistry.* 23:5570–5577.

Hui, S. W., T. P. Stewart, and P. L. Yeagle. 1980. Temperature dependent morphological and phase behavior of sphingomyelin. *Biochim. Biophys. Acta.* 601:271–281.

Hwang, S-b., C-s. C. Lee, M. J. Cheah, and T. Y. Shen. 1983. Specific receptor sites for 1-0-alkyl-2-acetyl-*sn*-glycero-3-phosphocholine (platelet activating factor) on rabbit and guinea pig smooth muscle membranes. *Biochemistry.* 4756–4763.

Levin, I. W. 1984. Vibrational spectroscopy of membrane assemblies. *In* Adv. Infrared and Raman Spectros. R. J. H. Clark and R. E. Hester, editors. John Wiley & Sons, Inc., New York. 1–48.

Mason, J. T., and C. Huang. 1981. Chain length dependent thermodynamics of saturated symmetric-chain phosphatidylcholine bilayers. *Lipids.* 16:604–608.

McManus, L. M., R. N. Pinckard, and D. J. Hanahan. 1983. Acetyl glyceryl ether phosphorylcholine (AGEPC) in allergy and inflammation. *In* Theoretical and Clinical Aspects of Allergic Diseases. H. Boström and N. Ljungstedt, editors. Almqvist and Wiksell International, Stockholm. 165–182.

Pinkard, R. N. 1983. Platelet-activating factor. *Hospital Practice.* 18:67–76.

Pinkard, R. N., L. M. McManus, and D. J. Hanahan. 1982. Chemistry and biology of acetyl glyceryl ether phosphatidylcholine (platelet activating factor). *In* Adv. in Inflammation Res. G. Weismann, editor. Raven Press, New York. 147–180.

Ruocco, M., and G. G. Shipley. 1982. Characterization of the subtransition of hydrated dipalmitoylphosphatidylcholine bilayers. *Biochim. Biophys. Acta.* 684:59–66.

Seelig, J. 1978. ^{31}P Nuclear magnetic resonance and the headgroup structure of phospholipids in membranes. *Biochim. Biophys. Acta.* 515:105–141.

Seelig, J., and A. Seelig. 1980. Lipid conformation in model membranes and biological membranes. *Q. Rev. Biophys.* 13:19–61.

Smith, I. C. P., and I. H. Ekiel. 1984. Phosphorous-31 NMR of phospholipid in membranes. *In* Phosphorous-31 NMR: Principles and Applications. D. G. Gorenstein, editor. Academic Press, Inc., New York. 447–475.

Snyder, R. G., S. L. Hsu, and S. Krimm. 1978. Vibrational spectra in the C–H stretching region and the structure of the polymethylene chain. *Spectrochim. Acta.* 34A:395–406.

Thayer, A. M., and S. J. Kohler. 1981. Phosphorous-31 nuclear magnetic resonance spectra characteristic of hexagonal aned isotropic phospholipid phases generated from phosphatidylethanolamine in the bilayer phase. *Biochemistry.* 20:6831–6834.

Wu, W., C. Huang, T. G. Conley, R. B. Martin, and I. W. Levin. 1982. Lamellar-micellar transition of 1-stearoyllysophosphatidylcholine assemblies in excess water. *Biochemistry.* 5957–5961.

Yeagle, P. L., W. C. Hutton, C. Huang, and R. B. Martin. 1975. Headgroup conformation and lipid-cholesterol associations in phosphatidylcholine vesicles: a ^{31}P(^{1}H) nuclear Overhauser effect study. *Proc. Natl. Acad. Sci. USA.* 72:3477–3481.